ORIGINAL ARTICLE

Keyhole welding with double-layer coaxial hybrid arc torch: a primary work

ZuMing Liu[1] · Fei Liu[1]

Abstract

Keyhole welding has an advantage in high efficiency, but the narrow process window for stable keyhole is a critical issue for application. Double-layer coaxial hybrid arcing technology is developed to decouple the heat and pressure properties in an arc source; this will improve the controllability of the weld pool thermal-force state. In this research, an arcing torch, designed by embedding an outer ring tungsten into the plasma arc nozzle to form a double-layer coaxial hybrid arc, was experimentally tested for its application possibility in the keyhole welding process. From the arc image and arc pressure results, stable hybrid arcing process was successfully achieved in the torch when the outer arc current is lower than 30 A. The arc pressure/current ratio in the outer arc current is about half to that in the center plasma arc current. Applying a 10-A outer arc current, keyhole welding can be achieved at a given center arc current of 110 A, which is lower than the threshold current for keyhole welding in an 8.3-mm thick 304 stainless steel plate. In the keyhole welding process in a 4.0-mm thick 304 stainless steel plate, keyhole behavior and the resultant weld have invisible change between the welding process with the hybrid arc torch and the ordinary plasma arc torch. The experimental test results give a promising method to improve the keyhole welding process window.

Keywords Keyhole welding · Welding torch · Plasma arc welding · Hybrid arc welding · Arcing behavior

1 Introduction

Welding process makes a joint between the workpieces; it is a very important fabrication technique for metal structure. Welding process has hundreds of types for different application fields. Among them, arc welding process is the most commonly used method because it has a simple device system and easy-going operation for different welding positions. Arc properties, especially the distribution of heat and force, play a key role to influence the welding process efficiency and the resultant weld quality as stated by Wu [1]. Modifying arc heat source is one of the most important works in the welding field.

An ordinary tungsten inert gas (TIG) arc has low current density and small arc pressure; narrow-depth weld pool and low-level welding speed restrict the overall manufacturing efficiency. With a high-energy density arc source, such as a constrained arc in plasma arc welding done in Yan's team [2] or high current arc in K-TIG welding as designed in Cui's team [3], melting depth will be much enhanced with a keyhole inside the weld pool. Keyhole is the gas–liquid interface between the plasma gas and the melted metal; the complex physical–chemical dynamic phenomenon is easily disturbed during the welding process, and keyhole stability is a key factor for the researcher or engineer as addressed in [4].

Numerous studies have been done in the aspects of process monitor, numerical model, and system modification as summarized in [5]. Keyhole state monitoring methods were developed with many types, for example, discharge voltage of the backside efflux plasma [6] or front side plasma cloud proposed by Zhang et al. in the University of Kentucky [7] and efflux plasma illumination light density proposed by He and Katsunori in JWRI Japan [8]. These methods can easily distinguish whether the keyhole opens or not. Vision sensing systems were developed by high-speed camera with additional laser illumination [9] or ordinary industrial camera with narrow-band filter glass [10]. Keyhole dynamic behavior was directly measured and related to the thermal state

✉ ZuMing Liu
   zuming.liu@tju.edu.cn

[1] School of Materials Science and Engineering & Tianjin Key Laboratory of Advanced Joining Technology, Tianjin University, Tianjin 300072, China
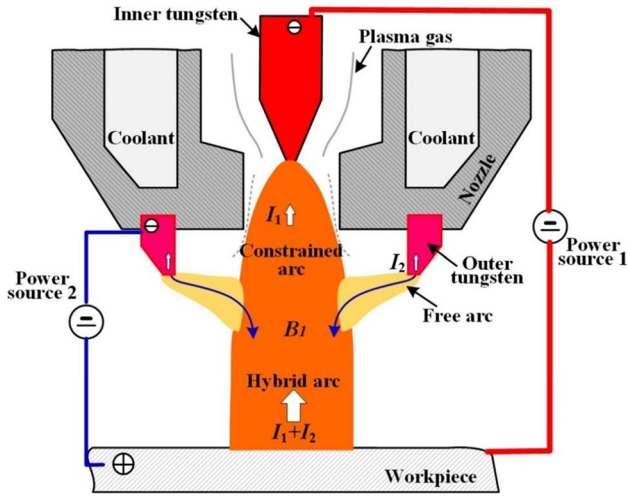
Fig. 1 Double-lay coaxial hybrid arc principle

of the weld pool [4]. These research results give comprehensive knowledge to understand the keyhole behavior and its stability and are the basic for the control system design. Numerical models were developed to simulate thermal-physical behavior in the keyhole weld pool. Among them, self-consistent model was developed to simulate the tungsten-nozzle-arc-keyhole-weld pool system by Jian et al. [11] in Wu's team. From the simulation results, keyhole behavior is the key to obtain stable welding process, and the force

and thermal state in weld pool should be carefully adjusted to guarantee keyhole stability. Torch modification is the most important work to meet the practical application. Stable arcing process is basic for keyhole welding. Additional modification in the torch focuses on the nozzle because the arc properties are highly related to the nozzle structure. Arc pressure of the constrained plasma arc is too heavy that force balance in the keyhole and weld pool is easily disturbed. Zhang et al. [12] designed a soft arc plasma arc torch by drilling two fine holes aside the center orifice throat, and the arc pressure weakens to stabilize the keyhole as observed in [13]. In Delft University of Technology, a radial gas flow was added around the center arc root to enhance the plasma arc power density by Hessel [14]. Li et al. [15] did a similar work in gas-focusing plasma arc welding, and stable keyhole welding process was achieved. In Wu's team, an ultrasonic vibration–assisted keyhole plasma arc welding was designed by Qiao et al. [16] to enhance the keyhole stability. All these modifications have effects to verify the arc properties and improve the keyhole stability to some degree. The torch system needs further modification to precisely control the arc properties and stabilize the keyhole process.

A novel modification based on plasma arc torch is developed to improve the arc properties' adjusting behavior. The arcing torch structure will be introduced, the arcing behavior will be measured in aspects of arc jet image and arc pressure

Fig. 2 a, **b** Arcing behavior (nozzle $\varphi 2.8$, arc length 10.0 mm)
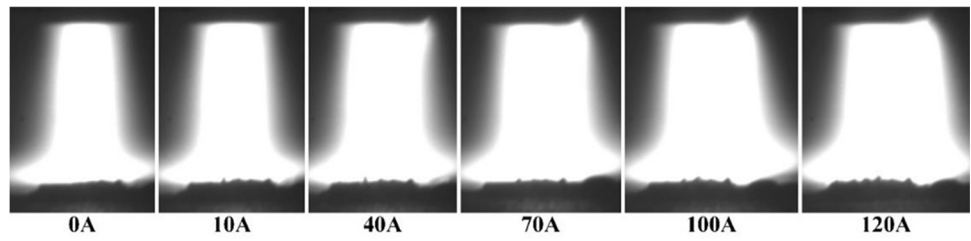
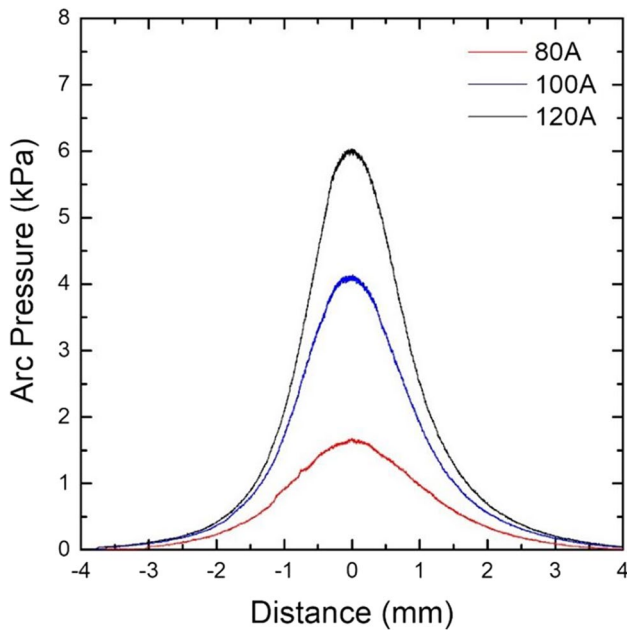(a) arc image (I_1=120A)
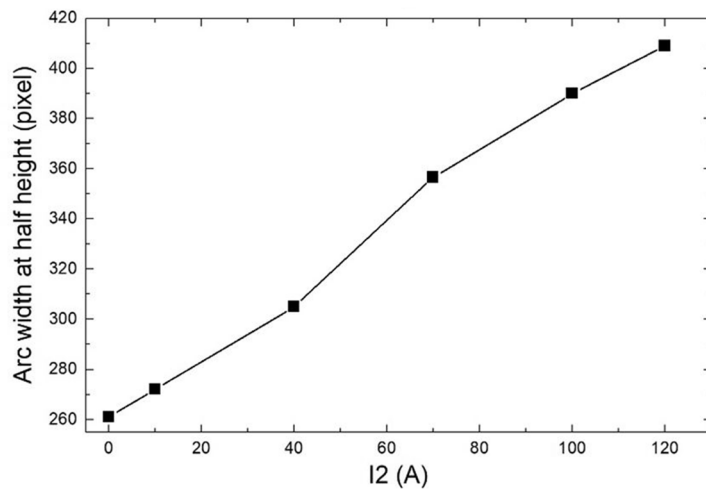
(b) arc width (I_1=120A)

Fig. 3 Arc pressure in constricted arc (nozzle φ2.8, arc length 10 mm, 2.6 L/min)

curve, and the keyhole welding process was experimentally tested. The results show that the novel torch gives a possibility to improve controllability of the keyhole stability.

2 Arcing torch structure and arcing system

As summarized in the above part, the systems in the ordinary or modified plasma arc torch have one-cathode-one-anode arcing system. In such a system, the arc force and heat properties are coupled in a given welding system. That is, when the welding current is changed, the arc force and heat will both be changed. Additionally, using a given welding system, the ratio of the arc pressure to the arc current is fixed. For example, the pressure/current ratio is small in the TIG system, while it is very high in an ordinary constrained plasma arc. If the force and the heat outputted in a single arc source is partially or fully decoupled, arc properties can be more adjusted with higher preciseness to control the thermal-force state in weld pool.

The proposed torch structure is diagrammatically shown in Fig. 1. It is modified based on a plasma arc welding torch. The arcing system for the constrained plasma arc, including weld power system, torch setup, gas flow, and coolant system, has no change. An outer ring tungsten is embedded in the bottom of the copper nozzle and is coaxially posited to the center orifice. An additional power source 2 is connected to the outer ring tungsten (negative terminal) and the workpiece (positive terminal) to form a ring-shaped free arc. The inner plasma arc and the outer ring free arc have the same current flowing direction. The inner arc is constrained by the

water-cooling copper nozzle, and the outer arc roots around the ring tungsten edge. The current density is much higher in the center constraint arc than in the outer free arc. The electromagnetic field density induced in the center constraint arc is so powerful that the less-power outer free arc will be attracted and absorbed into the center arc. In this way, a hybrid arc is created in the arcing system by coaxially positing an outer ring arc to a center constraint plasma arc. The arc current flows out from the workpiece into the hybrid arc and divides to two paths: one flows through the water-cooled
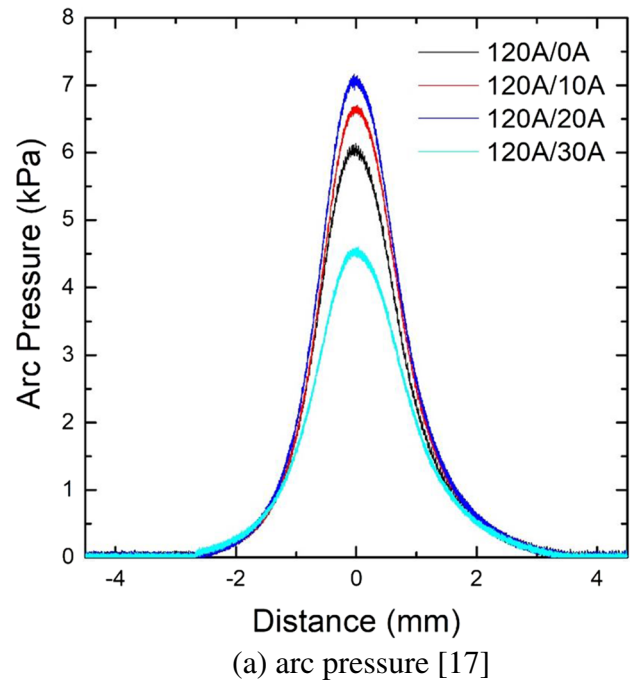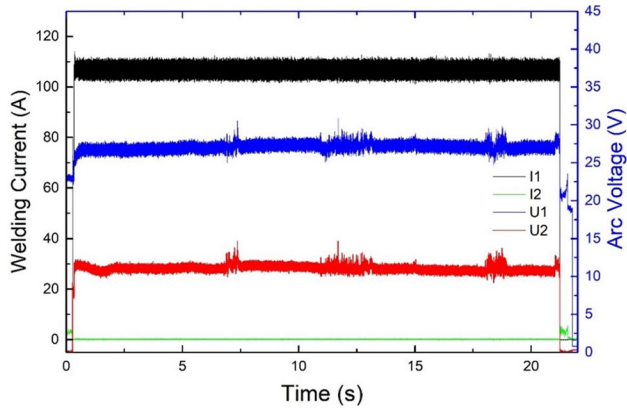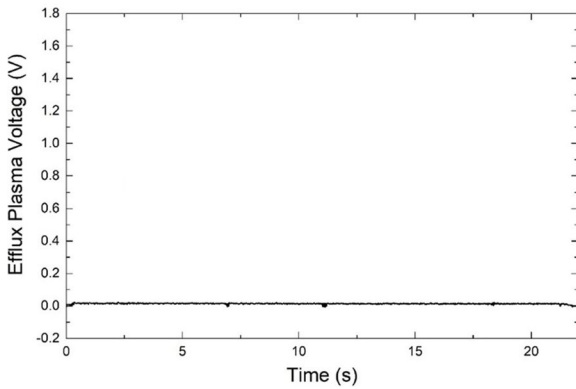

(a) arc pressure [17]
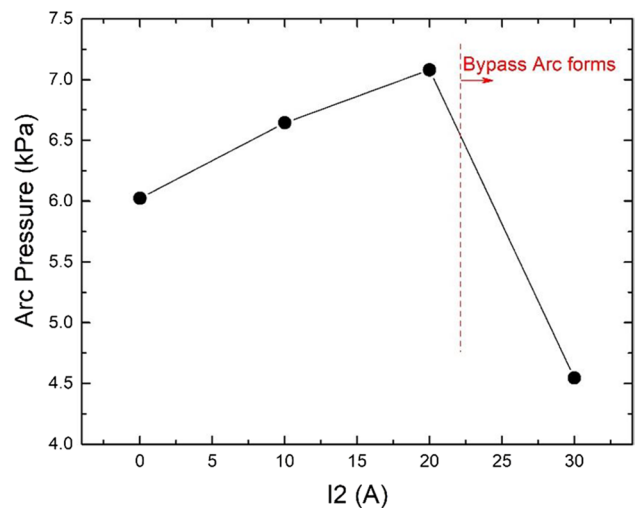
(b) peak pressure

Fig. 4 **a**, **b** Arc pressure (nozzle φ2.8, arc length 10.0 mm, 2.6 L/min, $I_1 = 120$ A)

(a) welding current and arc voltage

(b) efflux plasma voltage

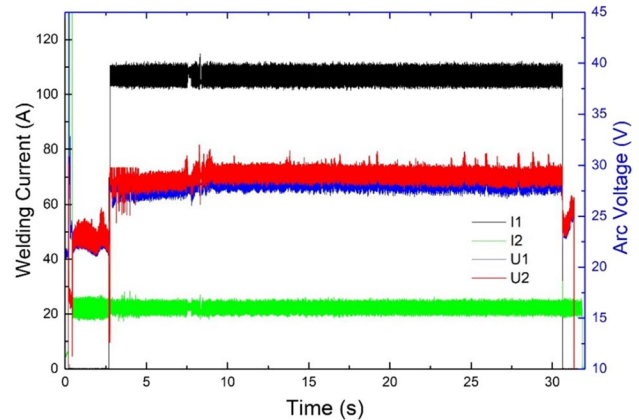**Fig. 5** **a**, **b** Electrical signals (I_1 = 110 A, I_2 = 0 A)

orifice into the inner tungsten acting as the constrained arc and the other flows into the ring tungsten as a ring free arc.

In the hybrid arcing system, two arc current paths flow into the hybrid arc: one is the center constraint arc current, marked as I_1, and the other is the outer free arc current, marked as I_2. The arc properties of the hybrid arc are related to the two arc current values. Because the current density is much lower in the free arc, the outer free arc has smaller pressure/current ratio compared with that in the constrained arc; the hybrid arc can hence be adjusted with higher pressure/current ratio by varying the constrained arc current or with lower pressure/current ratio by varying the free arc current as measured in the previous work [17]. That is, the arc pressure value of the hybrid arc is highly dependent on the current I_1 and less sensitive to the current I_2. The ratio of the arc pressure to the arc current will be not fixed in the proposed arcing system. In the constrained arc system, the arc pressure/current ratio can be adjusted by changing the nozzle orifice or varying the plasma arc gas, but the nozzle is fixed during the welding process; the gas flow rate is a sensitive factor for plasma arc pressure and it has delay. Changing the arc current has much better

convenience for adjusting the arc properties in real time. This is the key for a welding process control system.

As a result, during the welding process, the keyhole behavior can be controlled with higher precision in the developed hybrid arc welding system. In other words, as a keyhole forms at a set of process parameters, the force balance in the weld pool can be smoothly adjusted by changing the outer arc current. And, because the ratio of arc pressure to current is much less in the outer arc current, the process window for a stable keyhole welding should be widened. However, the experimental observation results show that the free arc is fully absorbed into the center arc to form a stable hybrid arc when the free arc current is less than 30 A, and it is unstable when the free arc current gets higher. During a practical welding process, the torch travels at the welding speed, and the situation differs to that in a stational spot arcing process, for example, the reflected plasma arc may influence the ring tungsten life. This is a primary work to verify the application possibility of hybrid arc torch into practical keyhole welding process.

In experiments, the arcing image and arc pressure curve were captured to evaluate the arcing stability and ratio of arc pressure to arc current. Keyhole welding process experiments are conducted to test whether stable keyhole welding
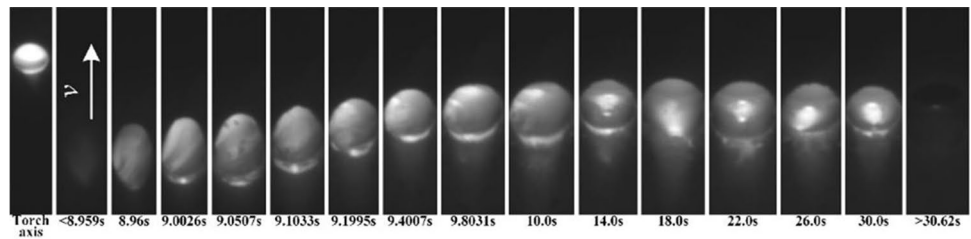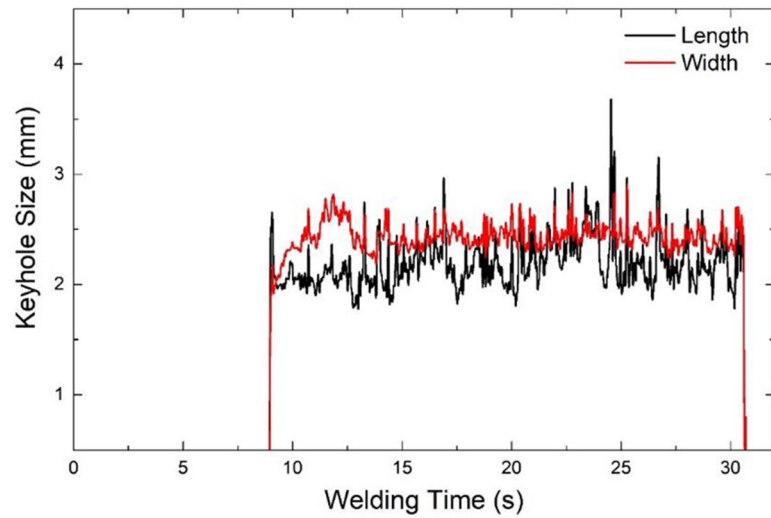

(a) welding current and arc voltage
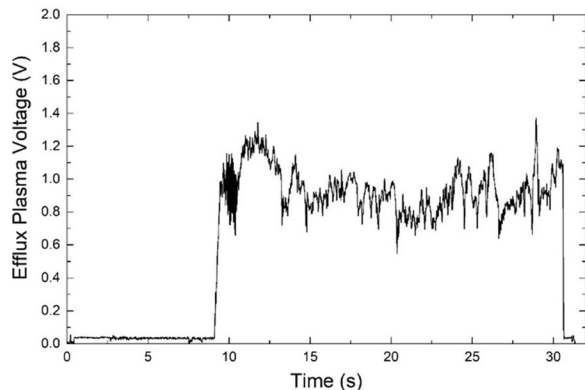
(b) efflux plasma voltage

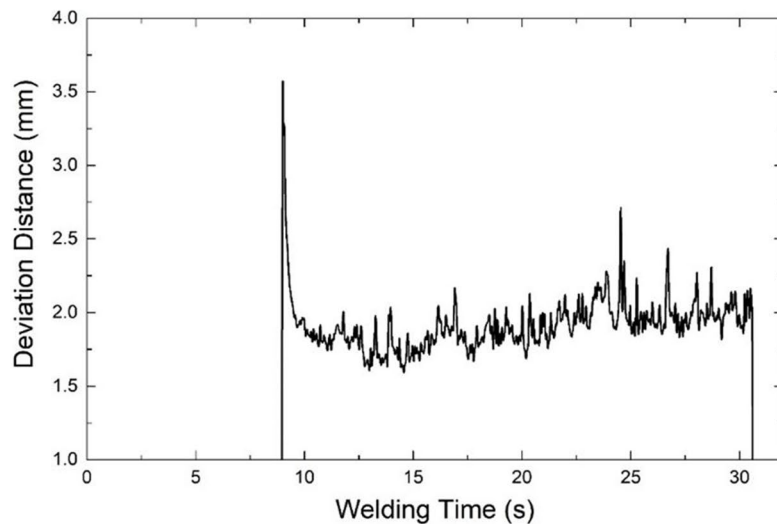**Fig. 6** **a**, **b** Electrical signals (I_1 = 110 A, I_2 = 20 A)

Fig. 7 **a–c** Keyhole process in PAW + TIG welding process (I_1 = 110 A, I_2 = 20 A) (8.3 mm thick SUS304, 120 mm/min, nozzle φ2.8, arc length 6.0 mm, I_1= 110 A, 3.0 L/min)

(a) Keyhole image (I_1=110A, I_2=20A)

(b) keyhole size

(c) keyhole deviation distance

process can be achieved or not by using the designed hybrid arc torch. In all experiments, the modified nozzle parameter such as the inner diameter of the ring tungsten (Ø 4.8 mm) is larger than the diameter of the nozzle orifice (Ø 2.8 mm), and the outer ring tungsten tip edge has a height of 2 mm from the nozzle bottom surface.

In the arcing system, the inner tungsten electrode rod was 4 mm in diameter with 60° tip angle, and the tungsten tip sets back 3 mm in the orifice throat from the bottom surface of the copper orifice. In the arcing process, pure argon is used as the plasma gas and shielding gas, and the flow rate of the shielding gas is 15 L/min.
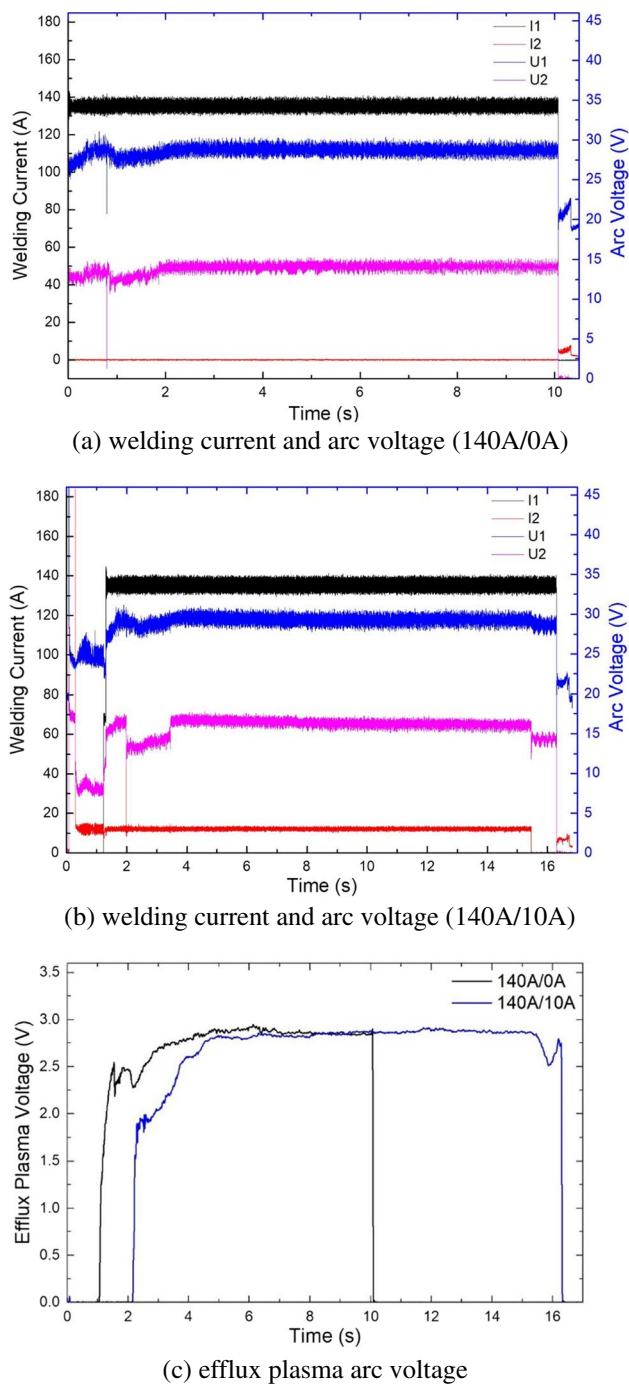
(a) welding current and arc voltage (140A/0A)

(b) welding current and arc voltage (140A/10A)

(c) efflux plasma arc voltage

Fig. 8 Welding process signals (4.0 mm thick SUS304, 240 mm/min, nozzle $\varphi 2.8$, arc length 6.0 mm, I_1= 140 A, 3.0 L/min)

3 Results and discussion

3.1 Arc image

Arc column image gives direct information of the arc burning behavior. In the first group of arc imaging test, the same current levels were applied with the torch height of 10 mm.

As shown in Fig. 2, the center constraint arc current is set at 120 A, and the outer ring arc current grows from zero to 120 A. The hybrid arc has a symmetry and bell-like shape when the current I_2 has a small level of 10 A, and point root arc takes place in the right side of the ring tungsten if the current I_2 further increases. The arc width at half the height increases nearly linear at an average slope of about 1.23 pixel/A.
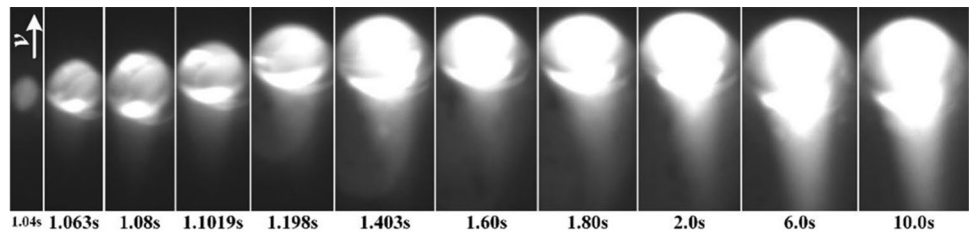
3.2 Arc pressure

Arc pressure curve is related to the flowing behavior in the arc column, and it is an important data to diagnose the arcing behavior. Pinhole method was used to measure the arc pressure curve. A pinhole with a diameter of 1.0 mm was drilled in the center of the water-cooled copper block, and a gas pressure sensor was coaxially equipped to the pinhole to sense the arc pressure. During the measuring process, the copper block is moving at a very slowly speed along the arc column diameter axis from one side to the other. The arc pressure along the arc diameter can be captured and recorded by the host computer. The arc pressure of the constrained arc and the hybrid arc was measured.

As shown in Fig. 3, the arc pressure curves of the constrained arc at currents of 80 A, 100 A, and 120 A are captured. The copper nozzle bottom offsets 10 mm from the workpiece surface, and the plasma gas flow rate is 2.6 L/min. All the three arc pressure curves have a symmetry and bell-like shape. The peak value increases from 1.66 kPa at 80 A to 4.11 kPa at 100 A and 6.0 kPa at 120 A. The average increasing slop of the arc pressure in a constrained arc is 108.5 Pa/A in this experiment.

For the hybrid arc, measurement experiments were carried out at a given current I_1 of 120 A. The torch height and the gas parameters are the same as used in Fig. 3. The outer layer arc current increased from 10 A to over 100 A. The captured arc pressure curves of current I_2 ranged in 0~30 A are shown in Fig. 4. All pressure curves distribute a symmetry and bell-like shape. As the outer ring arc current I_2 increases from 0 to 20 A, the pressure curves distribute nearly the same in the bottom half of the height or the radius region beyond 1.0 mm, and the core region grows following the current I_2. The peak value of the arc pressure curve grows up from 6.023 kPa at 120 A/0 A to 6.643 kPa at 120 A/10 A and 7.080 kPa at 120 A/20 A. The average increasing slope is 52.85 Pa/A by increasing current I_2. When the current I_2 gets 30 A, the hybrid arc pressure curve peak value drops heavily; this is because the nozzle is overheated by such a high ring arc current, and the center constraint arc stability is damaged, as analyzed in [17].

This gives a very important evidence that the ratio of pressure/current is just half of that by adjusting the outer free arc current than by adjusting the center constraint arc current. In
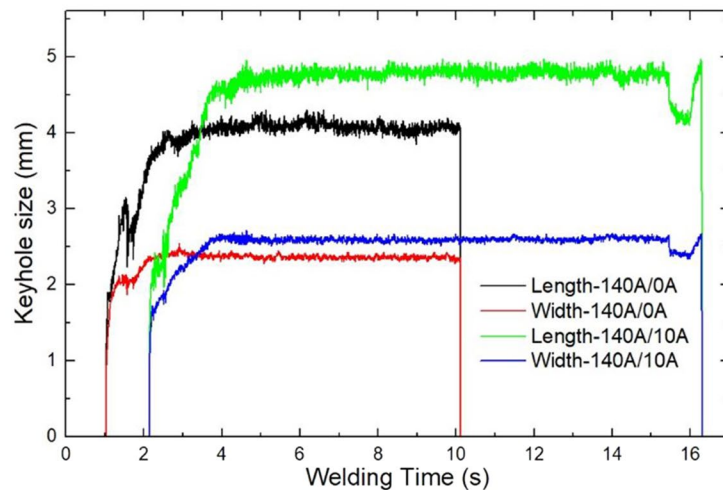
Fig. 9 a–c Keyhole behavior

(a) keyhole image (140A/0A)
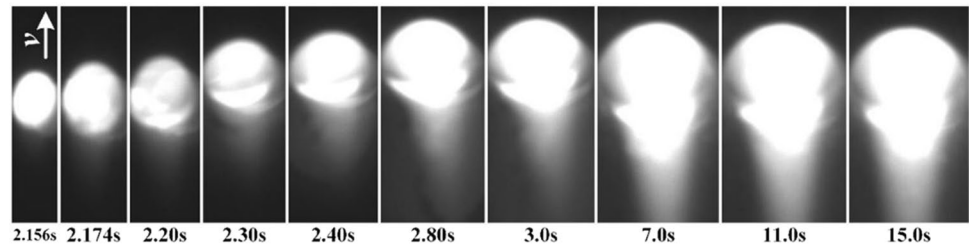
(b) keyhole image (140A/10A)

(c) keyhole size

other words, at a given constrained arc in the plasma arcing system, adjusting the outer free arc current value will give the anode zone a more smooth arc pressure change.

3.3 Keyhole welding process

In the keyhole welding process, keyhole forms in the fully melted weld pool, and keyhole wall is the gas–liquid interface. Such free interface behaviors highly dynamic at attacking of the arc plasma, balance between the arc force, surface tension, and gravity pressure give a key role to determine the keyhole stability. Controlling the arc pressure is a critical method to stabilize the keyhole. By using the novel arcing torch and setting the center constraint arc current to form the arc pressure high enough to form a keyhole in the fully melted weld pool, smoothly change the arc

pressure by adjusting the outer arc current value, which will need a wider range of current to create the same level of arc pressure. In other words, compared to the constrained arc as used in the plasma arc welding process, adjusting the outer arc current in the hybrid arc welding process will widen the current window for stable keyhole welding.

Here, we did two groups of keyhole welding experiments. Group 1 was conducted in an 8.3-mm thick SUS304 stainless steel plates, welding speed is 120 mm/min, the nozzle diameter is φ2.8 mm, the copper nozzle bottom offsets 6.0 mm to the workpiece, center arc current I_1 was set at 110 A, and the plasma gas flow rate is 3.0 L/min. Group 2 was conducted in a 4.0-mm thick SUS304 stainless steel plates, welding speed is 240 mm/min, the nozzle diameter is φ2.8 mm, the copper nozzle bottom offsets 6.0 mm to the workpiece, center arc current I_1 was set at 140 A, and the plasma gas flow rate is 3.0 L/min.
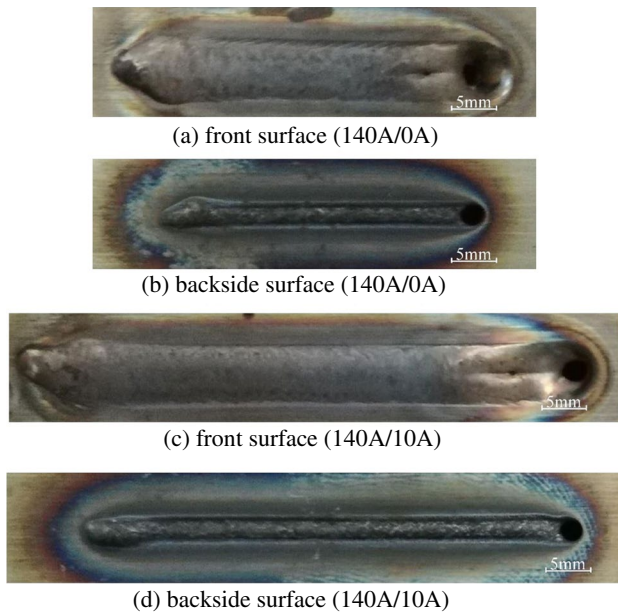
(a) front surface (140A/0A)

(b) backside surface (140A/0A)

(c) front surface (140A/10A)

(d) backside surface (140A/10A)

Fig. 10 **a–d** Weld surfaces

In the welding test group 1, two tests were done. As shown in Fig. 5, welding process was carried out with current I_1 at 110 A, the outer ring arc was not applied, and fully penetrated keyhole was not formed as diagnosed by the zero-level efflux plasma voltage curve. As shown in Fig. 6, current I_1 was set at 110 A, the outer ring arc was applied at current I_2 of 20 A, and fully penetrated keyhole was successfully formed as the efflux plasma voltage was observed to wave around 0.9 V. The arc voltage U_1 was voltage from the inner tungsten tip to the workpiece, and the arc voltage U_2 was measured from the outer ring tungsten tip to the workpiece. When the current I_2 was not applied, the voltage U_2 line is much lower under the voltage U_1 line. After the current I_2 was applied to successfully form a hybrid arc, the voltage U_2 line obviously goes up to the voltage U_1 level. The arc voltage U_1 level has invisible change after the current I_2 was applied. The thin gas film in the nozzle wall works as a robust electrical resistance between the center plasma arc and the copper nozzle when a stable hybrid arc forms.

Keyhole exit behavior was imaged with a backside camera as did in [10]. As shown in Fig. 7, during the welding process with I_1=110 A, I_2=20 A hybrid arc, keyhole experiences non-penetration (<8.96 s) and fully penetration keyhole stages. The keyhole also has an oval shape whose width is longer than the length. The keyhole exit deviation distance is very high at the keyhole open instance and then quickly goes down to the stable value. That is, keyhole behaviors in the hybrid arc welding process have invisible difference to those observed in the ordinary plasma arc welding. The developed nozzle works well during the long-time hybrid arc keyhole welding process.

In the second keyhole welding test group, the workpiece has 4-mm thickness, and the welding current and the welding speed are both increased. The welding processes were monitored, and the signals are shown in Fig. 8. In the 140 A/0 A and 140 A/10 A welding processes, fully penetrated keyhole forms. In the ordinary plasma arc welding process, the voltage U_2 is about 14.4 V, and it goes up to 16.4 V after the current I_2 was applied. While the center arc voltage is kept stable at about 29.4 V in the two testes, both tests achieved fully penetrated keyhole welding process as the efflux plasma arc voltage lines get about 2.86 V. That is, the keyhole stable state did not have visible difference between the hybrid arc process and the ordinary plasma arc welding process Fig. 9.

Keyhole exit behavior is imaged by the backside camera as shown in Fig. 8. In the two cases, keyhole exit first opens at a small size and then grows to the stable state, and keyhole exit position moves forward along the welding direction. Keyhole shape does not change much, but the keyhole size increases in the hybrid arc case (140 A/10 A). After image processing and camera calibration, keyhole parameters can be obtained. During the stable keyhole stage, keyhole width and length in case 140 A/10 A are 2.58 mm and 4.81 mm, respectively. The larger keyhole exit size phenomenon is related to the arc pressure that is enhanced in the hybrid arc; that is because the higher arc pressure acts to overcome the effect of gravity force and surface tension in the keyhole channel [18].

The weld surfaces obtained in the 140 A/0 A and 140 A/10 A keyhole welding tests are shown in Fig. 10. The two welds

Fig. 11 **a**, **b** Weld cross-sections
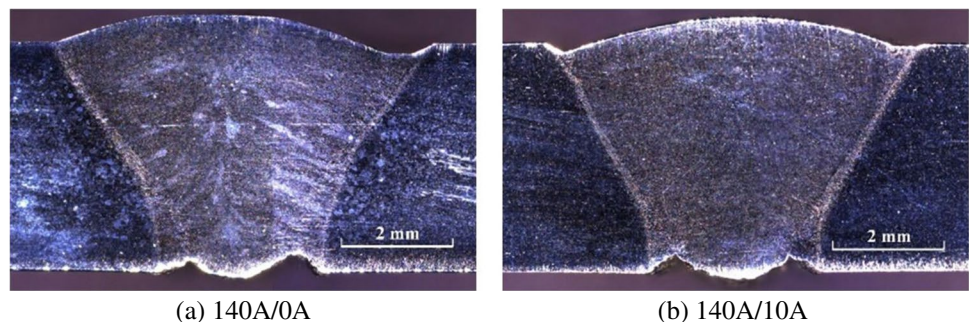
(a) 140A/0A

(b) 140A/10A

have smooth surface in the front and backside. The cross-section of the two welds, as shown in Fig. 11, have invisible change in the melting zone shape. The front weld width is 6.98 mm in 140 A/10 A and 6.89 mm in 140 A/0 A, and the backside weld width is 3.15 mm in 140 A/10 A and 3.09 mm in 140 A/0 A. That is, the weld width increases in the hybrid arc weld.

This is a primary try for this double-layer coaxial hybrid arc torch for keyhole welding process. Stable arcing process was successfully achieved with small level of outer free arc current, and the hybrid arc process will be damaged when the outer free arc current goes beyond about 30 A. And the fully penetrated keyhole welding process was successfully done with an outer free current of 10 A and 20 A by using the hybrid arc torch. The keyhole behavior and the resultant weld have invisible change in the research. Further modification of the study will improve the outer free arc current applied range, and a more comprehensive application test will be done for the hybrid arc torch.

4 Conclusions

(1) By embedding a ring tungsten electrode into the copper nozzle in a plasma arc torch, a novel hybrid arc torch is made. The ring free arc is fully absorbed into the center constraint arc to a hybrid arc. Stable hybrid arc was made with the outer arc current that is less than 30 A.

(2) The ratio of pressure/current in the outer ring arc is about half that in the constrained arc. The arc pressure peak value can be smoothly controlled by the outer free arc current.

(3) Keyhole welding was successfully achieved by using the hybrid arc torch at the outer arc current of 10 A and 20 A. The keyhole behavior has invisible change in the hybrid arc compared with in the ordinary constrained plasma arc.

This research gives a promising arcing method to adjust the arc pressure value by different pressure/current ratio. The current version can be applied in keyhole welding process for 30 s. Further modification of the torch structure should be done to improve the application range of the outer ring arc current.

Declarations

Conflict of interest The authors declare no competing interests.

References

1. Wu CS (2010) Welding thermal processes and weld pool behaviors. CRC Press

2. Yan ZY, Chen SJ, Jiang F, Zhang W, Huang N, Chen R (2020) Control of gravity effects on weld porosity distribution during variable polarity plasma arc welding of aluminum alloys. J Mater Proc Technol 282(8):116693

3. Cui SL, Liu ZM, Luo Z, Fang YX, Manladan SM, Yi S (2017) Keyhole process in K-TIG welding on 4mm thick 304 stainless steel. J Mater Proc Technol 243(5):217–228

4. Liu ZM, Wu CS, Liu YK, Luo Z (2015) Keyhole behaviors influence weld defects in plasma arc welding process. Weld J 94(9):281-s-290-s

5. Liu ZM, Cui SL, Luo Z, Zhang CZ, Wang ZM, Zhang YC (2016) Plasma arc welding: process variants and its recent developments of sensing, controlling and modeling. J Manuf Proc 23(8):315–327

6. Zhang SB, Zhang YM (2001) Efflux plasma charge-based sensing and control of joint penetration during keyhole plasma arc welding. Weld J 80(2):157–162

7. Zhang YM, Zhang SB, Liu YC (2001) A plasma cloud charge sensor for pulse keyhole process control. Meas Sci Technol 12:1365–1370

8. He DF, Katsunori I (1984) Penetration-self-adaptive free-frequency pulsed plasma arc welding process controlled with photocell sensor. Trans JWRI 13(1):7–11

9. Zhang YM, Zhang SB (1999) Observation of the keyhole during plasma arc welding. Weld J 78:53-s-58-s

10. Liu ZM, Wu CS, Chen MA (2014) Experimental sensing of the keyhole exit deviation from the torch axis in plasma arc welding. Inter J Adv Manuf Technol 71:1209–1219

11. Jian XX, Wu CS (2015) Numerical analysis of the coupled arc–weld pool–keyhole behaviors in stationary plasma arc welding. Int J Heat Mass Tran 84:839–847

12. Zhang QL, Yang CL, Lin SB, Fan CL (2014) Novel soft variable polarity plasma arc and its influence on keyhole in horizontal welding of aluminum alloys. Sci Technol Weld Join 6:493–499

13. Zhang QL, Yang CL, Lin SB, Fan CL (2015) Soft variable polarity plasma arc horizontal welding technology and weld asymmetry. Sci Technol Weld Join 4:296–306

14. Hessel LV (2014) Increased power density plasma arc welding. Master thesis, Delft University of Technology

15. Li TQ, Yang XM, Chen L, Zhang Y, Lei YC, Yan JC (2020) Arc behavior and weld formation in gas focusing plasma arc welding. Sci Technol Weld Join 25(4):329–335

16. Qiao JN, Wu C, Li YF (2020) Numerical and experimental investigation of keyholing process in ultrasonic vibration assisted plasma arc welding. J Manuf Proc 50:603–613

17. Liu ZM, Liu F, Zhao XC (2022) A novel arc plasma generating method by coaxial hybrid a ring arc to constraint arc: principle and progress. J Manuf Process 82(10):362–373

18. Xu B, Chen SJ, Tashiro S (2021) Physical mechanism of material flow in variable polarity plasma arc keyhole welding revealed by in-situ x-ray imaging. Phys Fluids 33(1):17121